Current status of the Hobby-Eberly Telescope wide field upgrade and VIRUS

Savage, Richard, Booth, John, Gebhardt, Karl, Good, John, Hill, Gary, et al.

Richard D. Savage, John A. Booth, Karl Gebhardt, John M. Good, Gary J. Hill, Phillip J. MacQueen, Marc D. Rafal, Michael P. Smith, Brian L. Vattiat, "Current status of the Hobby-Eberly Telescope wide field upgrade and VIRUS," Proc. SPIE 7012, Ground-based and Airborne Telescopes II, 70120B (10 July 2008); doi: 10.1117/12.789360

SPIE.

Event: SPIE Astronomical Telescopes + Instrumentation, 2008, Marseille, France

Current Status of the Hobby-Eberly Telescope Wide Field Upgrade and VIRUS

Richard D. Savage, John A. Booth, Karl Gebhardt, John M. Good, Gary J. Hill, Phillip J. MacQueen, Marc D. Rafal, Michael P. Smith, Brian L. Vattiat

McDonald Observatory, The University of Texas at Austin, 1 University Station C1402, Austin, TX, USA 78712-0259

ABSTRACT

The Hobby-Eberly Telescope (HET) is an innovative large telescope of 9.2 meter aperture, located in West Texas at the McDonald Observatory. The HET operates with a fixed segmented primary and has a tracker which moves the four-mirror corrector and prime focus instrument package to track the sidereal and non-sidereal motions of objects. A major upgrade of the HET is in progress that will substantially increase the field of view by replacing the corrector, tracker and prime focus instrument package. In addition to supporting the existing suite of instruments, this wide field upgrade will feed a revolutionary new integral field spectrograph called VIRUS, in support of the Hobby-Eberly Telescope Dark Energy Experiment (HETDEX). This paper discusses the current status of this upgrade.

Keywords: Hobby-Eberly, HET, HETDEX, Spectrograph, VIRUS, IFU, Telescope

1. INTRODUCTION

The Hobby-Eberly Telescope (HET) was originally envisioned as a spectroscopic survey telescope, able to efficiently survey objects over wide areas of the sky. While the telescope has been very successful observing large samples of objects such as quasi-stellar objects (QSOs) spread over the sky with surface densities of around one per 10 sq. degrees, the HET design, coupled with a small field of view corrector, hampers programs where objects have higher sky densities. In seeking a strong niche for the HET going forward, the HET field of view will be increased from 4′ to 22′ so that it can accommodate the Visible Integral-field Replicable Unit Spectrograph (VIRUS), an innovative, highly multiplexed spectrograph that will open up the emission-line universe to systematic surveys for the first time, uncovering populations of objects selected by their line emission rather than by their continuum emission properties.

The Hobby-Eberly Telescope (HET) will undergo this major upgrade in 2010 to support the HET Dark Energy Experiment (HETDEX) as well as current and future instrumentation. This upgrade project (referred to as the HETDEX project, or just HETDEX) consists of three primary elements:

- HET wide field upgrade (WFU)
- Design, fabrication and deployment of VIRUS on HET
- Execution of the Dark Energy Experiment[1] (DEX) survey with the VIRUS on HET

The primary goal of HETDEX is to meet the science requirements for the DEX while preserving and/or improving upon HET's current capabilities. Science requirements for HETDEX were scrutinized at the Science Requirements Review (SRR) in June 2007. This was followed by a Preliminary Design Review (PDR) in April 2008 which scrutinized the technical requirements that "flowed down" from the science requirements. Both independent review panels found HETDEX to be scientifically compelling, technically feasible and programmatically sound. Additionally, the PDR review panel declared the project to be ready to move to the next phase. HETDEX is currently at the beginning of the detailed design and fabrication phase. Over the next two years, designs will be finalized, hardware manufactured and assembled, and the system integrated and thoroughly tested prior to installation and commissioning in the fall of 2010.

A brief review of the HET is presented in Section 2 so that the reader can better appreciate the differences between the current and upgraded system designs. This is followed by a high-level look at some of the more mature aspects of the system design that were presented at the PDR. Discussions related to software and computer hardware have been omitted due to space limitations.

Ground-based and Airborne Telescopes II, edited by Larry M. Stepp, Roberto Gilmozzi,
Proc. of SPIE Vol. 7012, 70120B, (2008) · 0277-786X/08/$18 · doi: 10.1117/12.789360

2. BACKGROUND

2.1 HET History and Description

The HET is located in West Texas at the McDonald Observatory on Mt. Fowlkes. It was funded and built by a consortium of five universities, the University of Texas at Austin, the Pennsylvania State University, the Ludwig-Maximilians Universität München, the Georg-August-Universität Göttingen, and Stanford University. HET was originally conceived in the early 1980s as the Penn State Spectroscopic Survey Telescope.[2] The name was later changed to the HET in 1989. Groundbreaking started at the observatory in March 1994 and commissioning started in 1997.[3] HET has been in continual service ever since science operations began in October 1999.

The HET (Figure 1) is an innovative telescope with an 11 m hexagonal-shaped spherical mirror comprising 91 identical 1 m hexagonal segments that are supported by a steel truss. The mirror has a 26164 mm radius of curvature and sits at a fixed zenith angle of 35°; it can be moved in azimuth to access about 70% of the sky visible at the observatory. Images of astronomical objects are acquired and followed across the spherical focal surface of the primary mirror by means of a tracking device (referred to as the tracker) which is mounted on top of the telescope (Figures 1 and 2). The tracker carries the prime focus instrument package (PFIP) so that its optical axis remains normal to and on the focal sphere of the primary mirror at all positions. The PFIP contains a variety of different instruments (see below) as well as a spherical aberration corrector (SAC), which corrects the incoming wave-front from the primary mirror and forms an image of the sky. The SAC is a four-mirror double-Gregorian type corrector that is designed to produce images with a FWHM < 0.6″ in the absence of seeing, over a 4′ (50 mm) diameter science field of view. It has a 9.2 m diameter pupil, that sweeps over the primary mirror as the tracker follows objects from between 41 minutes (in the south at δ = -11°) and 39 minutes (in the north at δ = +72°). The maximum track time per night is 2.8 hours and occurs at +67°.

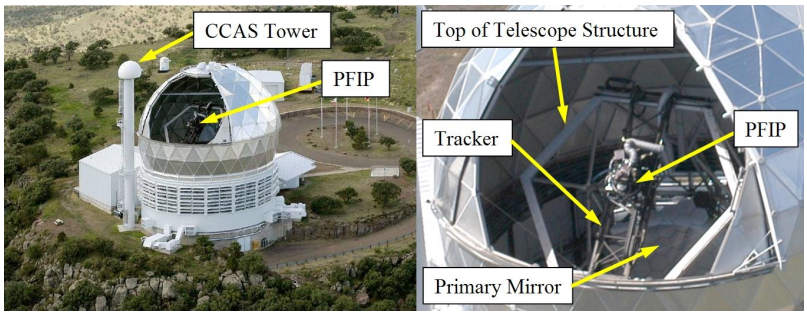

Figure 1. The figure on the left shows the HET with the dome shutter open. The figure on the right is a close up view of the top of the HET revealing the telescope structure which supports the tracker and PFIP.

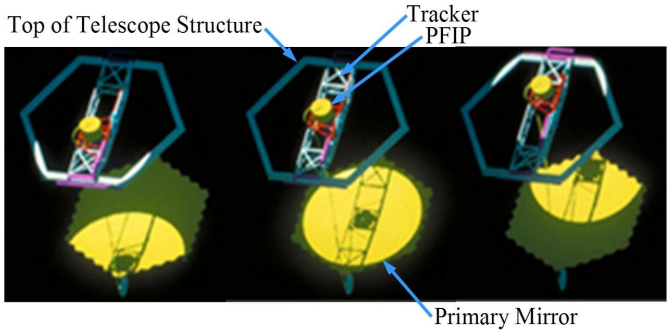

Figure 2. The tracker allows the PFIP to follow objects across the sky. A moving baffle at the exit pupil of the SAC is used to baffle the variable unfilled part of the pupil that occurs during tracking.

The HET science instruments[4] are the Marcario low resolution spectrograph (LRS), the medium resolution spectrograph (MRS), and the high resolution spectrograph (HRS). The LRS rides in the PFIP on the tracker, allowing it to image as well as take spectra. It is fed by a fold mirror, for a total of six reflections to reach the LRS slit. The MRS and HRS are installed in the spectrograph room which is located in the basement under the telescope, internal to the pier. These spectrographs are fiber fed from the fiber instrument feed (FIF) that is part of the PFIP. The FIF is fed directly from the SAC focal surface without further reflection.

2.2 HET Operation

The HET is operated 365 nights per year under normal West Texas outdoor conditions, shielded from the wind somewhat by the surrounding dome structure. During the day, the dome interior is air conditioned to the expected nighttime opening temperature to offset solar heating.

Prior to starting an observing run, HET's mirror alignment recovery system (MARS)[5] is used to ensure that all of the primary mirror segments are aligned in tip and tilt relative to one another. This process, known as "stacking," is accomplished with the help of a Shack Hartmann-based sensor that is located at the spherical mirror's desired center of curvature, which is located in the center of curvature alignment sensor (CCAS) tower adjacent to the HET dome (Figure 1). MARS automatically sets the tip and tilt of each mirror segment based upon measurements made with the Shack Hartmann sensor. After all segments are aligned, the segment alignment maintenance system (SAMS)[6] automatically maintains segment alignment for extended periods.

An observation is initiated by rotating the entire telescope structure to the desired azimuth and then using the tracker to slew the PFIP to the starting position selected by the resident astronomer (RA). During the observation, the tracker automatically moves the PFIP to track the image (formed by HET's stationary primary mirror) as it moves across the primary mirror's spherical focal surface. Motion along six axes (X, Y, W, θ, Φ, and ρ, as shown in Figure 3) is required to track and maintain the SAC's optical axis normal to and on the primary mirror spherical focal surface at all positions along the track.

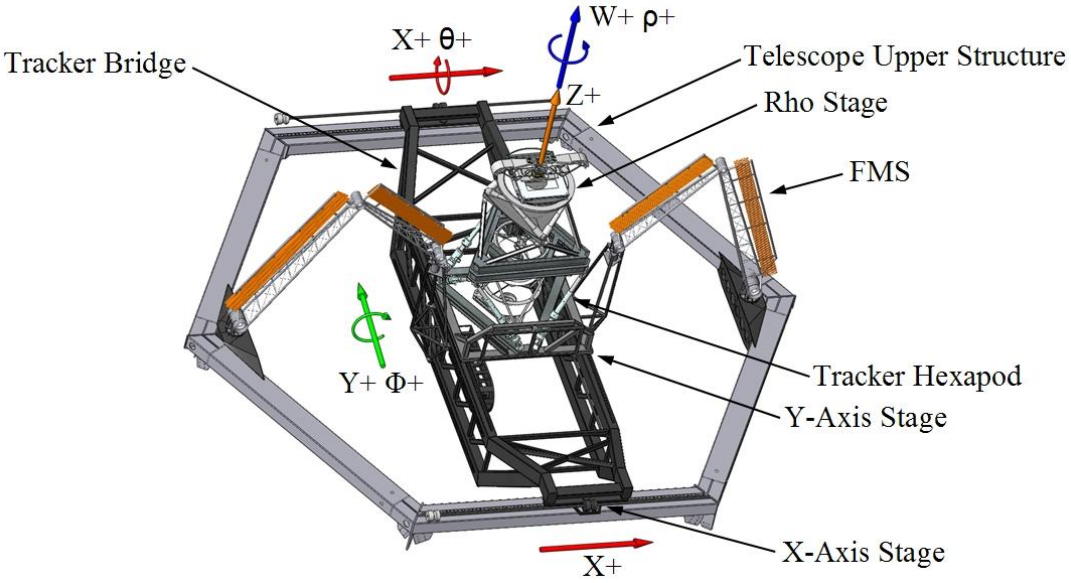

Figure 3. This figure depicts the tracker coordinate system with the PFIP in its central position. (Note that this figure shows the new tracker and PFIP as described in Sections 3.2 and 3.3 below.) The Z and W axes are coincident when the PFIP is in its central position. As the PFIP moves away from its central position, the angle between the Z and W axes increase. Note that the X, Y and Z axes are orthogonal to one another, the Z axis is coincident with the primary mirror optical axis, and the positive direction for θ, Φ and ρ is based upon the right-hand rule. Also note that the angle between the W and Z axes is referred to as β (and is not shown in this figure).

Requisite motions are achieved (under closed loop control using the metrology equipment described in Section 3.2) with the tracker's X-Y stage, hexapod and rho stage (Figure 3). The X-Y stage translates the PFIP in a plane perpendicular to the primary mirror's optical axis, while the hexapod translates the PFIP along the SAC's optical axis (i.e., the W axis) to maintain focus. The hexapod also tips (θ) and tilts (Φ) the PFIP (i.e., rotates it about the X and Y axes, respectively) to keep the SAC's optical axis normal to the primary mirror's focal surface. Tipping and tilting (by as much as ±8.5° about the 35° zenith angle of the optical axis) occurs around the SAC's stationary-image rotation point (SIRP) near the circle of least confusion of the primary mirror. Rotation about the SIRP changes the coma of the optical system while not moving the image on the corrector's focal surface. The rho stage is used to compensate for field rotation by rotating the SAC and HET science instruments and metrology equipment about the ρ axis.

2.3 HET Current Status

In early operations, typical image quality was between 2″ and 3″ FWHM.[4,7,8] Since then a variety of projects[9,10,11,12] were completed to improve image quality. This included development of MARS, SAMS, DMI and TTCAM, as well as improvements to the dome ventilation system. In the first quarter of 2008, HET had a median image quality of 1.8″ FWHM, which included 1.2″ FWHM site seeing as measured by the observatory's differential image motion monitor.[13]

3. HET WIDE FIELD UPGRADE

The WFU[4,10] will improve system performance and add new capabilities (Table 1). This will be accomplished by designing, fabricating, and deploying a larger field of view corrector (referred to as the wide field corrector [WFC]) that will replace the existing SAC. It also requires design, fabrication, and deployment of a new PFIP and tracker, as well as modification to the HET's azimuth bearings, to accommodate additional weight being added to the telescope.

Table 1. Anticipated HET improvements offered by the WFU.

1	Significantly larger field of view
2	Higher throughput offered by larger pupil and better mirror coatings
3	Better environmental protection for the WFC mirror coatings via air purge system
4	Better image quality due to improved control system and additional metrology equipment
5	ADC for atmospheric dispersion compensation
6	Optical bench instrument changer accommodates additional science instruments
7	Improved telescope observing efficiency by reducing overheads associated with pointing and focusing
8	Allows the HET to accommodate 192 spectrographs to facilitate systematic emission-line surveys of the universe

3.1 Wide Field Corrector

In mid-2007 two parallel study contracts were issued to Sagem Défense Sécurité[14] and the University of Arizona Optical Sciences Center[15] to better understand the WFC requirements, performance envelope, and cost. These studies were completed in July 2007. The starting point for each study was the baseline design developed by Phillip MacQueen which is described in Reference 16. The conclusion of both study efforts was that the WFC is a challenging but realistic design that can be built in about two years by a focused and competent contractor. The WFC procurement process is currently underway, with anticipated delivery in Summer 2010. The procurement specification is based upon the reference design (Figure 4) that resulted from the two studies.

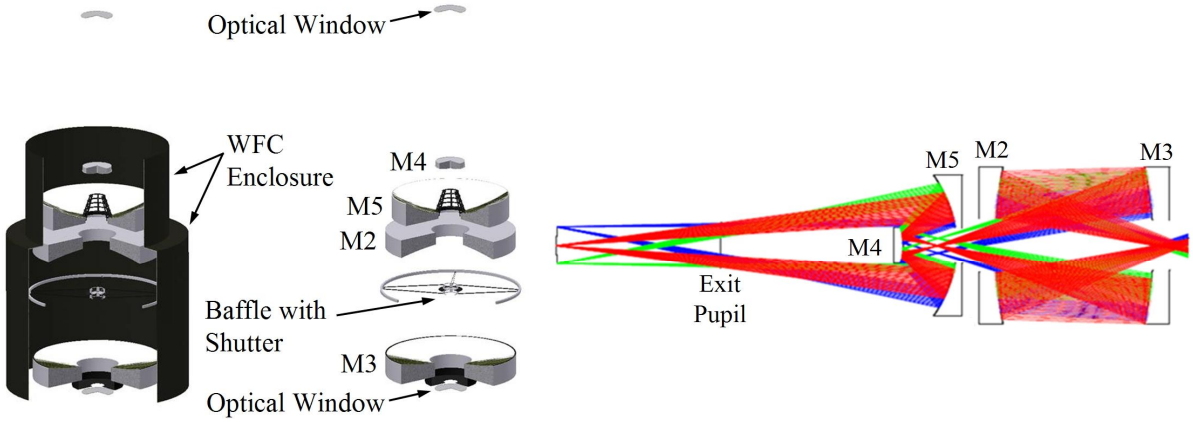

Figure 4. The figure on the left shows views of the WFC and optical components. Along the vertical axis from the bottom up, the elements are the ENWA optical window (only W1 is shown), input field stop (black), M3 facing upward, the axial baffle with shutter on a notional spider support, M2 facing downward, M5 facing upward with baffle, M4 facing downward, and finally, the EXWA optical window (only W3 is shown). The figure on the right is a ray trace of the reference design excluding the ENWA, EXWA and primary mirror. The primary mirror is approximately 12 m to the right of the figure and concave toward the corrector. The WFC focal spherical surface is to the left. It is concave with a radius that is on the order of 1 m.

The reference design is a four-mirror design with two concave 1 m diameter mirrors, one concave 0.9 m diameter mirror, and one convex 0.23 m diameter mirror. Since the corrector is designed for feeding optical fibers at f/3.65 the chief ray from all field angles is normal to the focal surface. This is achieved with a concave spherical focal surface centered on the exit pupil. The primary mirror spherical aberration and the off-axis aberrations in the wide field are controllable due to the first two mirrors being near pupils, and the second two mirrors being well separated from pupils. The aberration balance in the baseline design favors image quality in the outer field over on-axis performance. This is because most of the field area is in the outer field, and also for the following reason: the segmented primary mirror of the HET is not phased, and so the diffraction-based performance of the HET is determined by its 1 m diameter primary mirror segments; therefore the on-axis performance of the baseline design need only be constrained to be comparable to the diffraction limit of a single primary mirror segment.

The reference design produces a 22′ diameter science field of view with a 10 m diameter pupil. Image quality without atmospheric dispersion correction is specified to be ≤ 0.45″ EE80 from the center of the WFC's optical axis out to a 5′ field angle radius and then increasing linearly to ≤ 0.80″ EE80 an 11′ radius.

The WFC consists of a variety of optical elements and baffles that are contained within a rigid enclosure that attaches to the PFIP via a kinematic mount. The optical entrance and exit of the WFC enclosure are covered by window assemblies that protect the WFC's internal components from the exterior environment. Since the window assemblies do not provide an airtight seal, the entire enclosure is purged with dry filtered air (instrument air) to prevent ingress of contaminants and to keep the interior of the WFC within 0.2°C of the ambient air temperature. Note that the air temperature, humidity and flow rate will be continually monitored to ensure they are within acceptable limits. Additionally, the exhaust line is equipped with a relief valve to prevent over pressurization and an electronic pressure sensor to monitor pressure.

The window assembly located at the WFC's optical entrance is referred to as the entrance window assembly (ENWA). This assembly is mounted directly to the WFC enclosure which supports its entire mass. The window assembly located at the WFC's optical exit is referred to as the exit window assembly (EXWA). This assembly interfaces to the WFC via a light-tight bellows. The EXWA is supported by the PFIP (see Figure 5) and not by the WFC's rear structure. This design feature improves WFC image quality because it eliminates potential optical element misalignments caused by the mass of the EXWA.

A ray trace of the WFC reference optical design is shown in Figure 4. Photons reflected from the primary mirror (M1) enter the WFC through the ENWA. The ENWA is used to support metrology equipment (DMI, TTCAM, and a facility calibration unit [FCU] which contains a variety of calibration lamps) and to deploy a set of two interchangeable thin optical windows (W1 and W2) that are mounted to a computer-controlled stage. This two-position stage allows W1 and W2 to be interchanged. Each of these windows is optimized for high transmission throughput over a particular bandwidth. W1 is optimized for the shorter wavelength bandwidth range, while W2 is optimized for the longer wavelength bandwidth range.

Photons passing through the ENWA are reflected from mirrors M2, M3, M4 and M5, respectively. These mirrors are used to correct the incoming wave-front from the spherical primary. The coatings on these mirrors are optimized to achieve maximum throughput from 350 nm to 1800 nm.

Photons reflected from M5 exit the WFC through the EXWA. The EXWA consists of a moving baffle (MB), two thin optical windows (W3 and W4) and an atmospheric dispersion compensator (ADC). The optical windows and the ADC are mounted to a computer-controlled stage. This three-position stage allows W3, W4 and the ADC to be interchanged. Each of these windows is optimized for high transmission throughput over a particular bandwidth. W3 is optimized for the same bandwidth range as W1, and W4 is optimized for the same bandwidth range as W2. The ADC is optimized for the wavelength range of 350 nm to 1100 nm.

The MB is mounted directly below the three-position stage at the exit pupil to baffle the variable unfilled part of the pupil that occurs during star tracking. The pupil becomes unfilled as the optical axis of the WFC points away from the center of the primary mirror during a track (see Figure 2).

Photons exiting the EXWA travel toward the WFC focus where they form a 22′ diameter image of the sky. The central portion of the field of view is reserved for science instruments and has a diameter of at least 18′. This is the field diameter required by the baseline distribution of the optical fibers (referred to as integral field units) feeding VIRUS (see Figure 9). The annular region surrounding this central region has a diameter of at least 22′, and is available to sensors which provide signals for closed-loop positional control of the tracker.

The WFC will be equipped with baffles to control stray light. The reference design has a baffle that is located between M2 and M3. The center of the baffle contains a small circular aperture that is used to facilitate optical alignment of the WFC with respect to the other telescope optics. A computer-controlled shutter is used to block the circular aperture when the telescope is in use. In general, all baffles that block light travelling along the WFC optical axis will need to be equipped with computer-controlled shuttered apertures to facilitate optical alignment.

Field rotation compensation is currently achieved by using the rho stage to rotate the SAC and HET science instruments about the ρ axis. In the upgraded system, the WFC will be mounted below the rho stage so that it does not rotate during field compensation. This will simplify the design and should help improve image quality because it eliminates rotation-induced stress reversals in the WFC mechanical support structure.

Experience obtained in commissioning the HET and its sister telescope, the South African Large Telescope, strongly suggests that the WFC needs to be thoroughly tested as an integrated unit while subjected to the same gravity vectors that will be encountered during deployment. This experience also suggests that the observatory must possess a means to test the WFC's internal optical alignment at the observatory (preferably while on the telescope) to facilitate troubleshooting during installation and testing, as well as years later during WFC reassembly after its mirrors have been recoated. Even though these requirements are expensive to meet, they are considered essential (to mitigating schedule risk during installation and commissioning) and are included in the supplier's scope of work for the WFC.

3.2 New PFIP

A new PFIP is required to support the larger and heavier WFC, ADC, optical bench, and additional metrology equipment. The PFIP is show in Figure 5 with a full field ADC. A lower cost partial field ADC for MRS and HRS is also being explored.

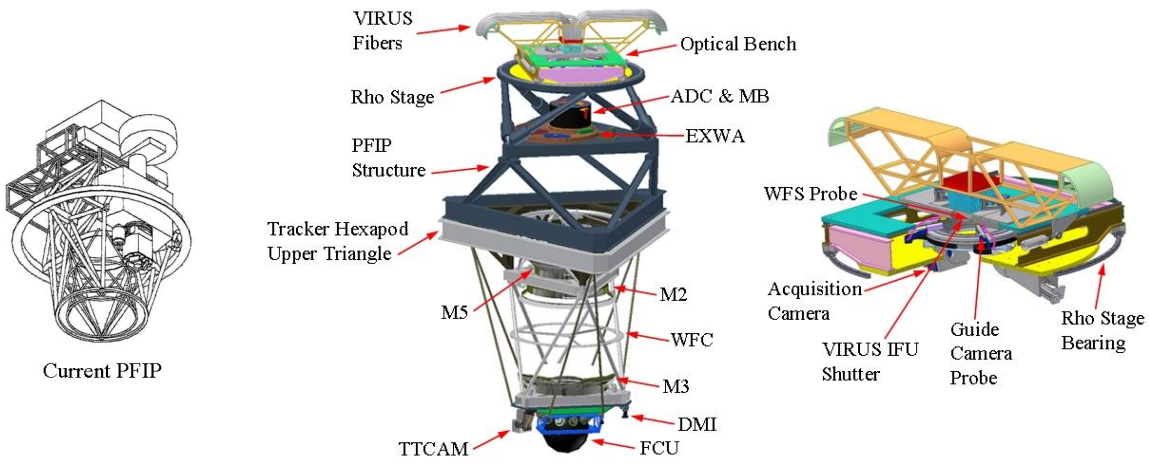

Figure 5. This figure shows the current and new PFIP approximately to scale. The solid model in the middle shows the current design of the PFIP with light-tight covers removed to show its primary components. The FCU (at the bottom of the PFIP) is mounted on a linear slide and is shown in its deployed position. The solid model on the right shows a close-up of the optical bench which rests on top of the rho stage.

The optical bench, which is located at the top of the PFIP, rests on the rho stage. It is equipped with an instrument changer (i.e., a pneumatically-actuated linear slide) which allows the RA to select between two different suites of science instruments. The first suite is reserved for the VIRUS integral field units (IFUs) and non-steerable FIFs for LRS, MRS and HRS. The second suite is reserved for metrology equipment that will be used during installation and commissioning of the upgraded telescope, and for future steerable FIF probes for LRS, MRS and HRS.

During a track, the tracker attempts to hold the corrector and PFIP at the correct orientation and location in track space under closed loop control while SAMS attempts to hold the primary mirror figure. Closed-loop control feedback is currently provided by a distance measuring interferometer[17] (DMI, which measures the distance between the primary mirror and WFC), a tip-tilt camera[17] (TTCAM, which measures the angular orientation [i.e., tip and tilt] of the WFC with respect to the primary mirror), a single guide camera (which is used for guiding in right ascension and declination), and hundreds of inductive edge sensors on the primary mirror segments. The WFU adds additional sensors (i.e., another

guide camera and two Shack-Hartmann wave-front sensors[18] [WFSs]), and a global radius of curvature (GROC) control loop, to provide redundancy on all controlled axes. It also allows the system to automatically maintain rotation, focus, and GROC/plate scale as indicated in Table 2.

Table 2. Upgraded HET control system sensors and functions where S = Sense and C = Control.

Function	Guiders	WFSs	DMI	TTCAM
Position on sky (x, y)	S, C			
Rotation	S, C			
Focus		S, C	S, C	
Primary mirror GROC/plate scale	S	S, C	S, C	
Tip/tilt of corrector		S		S, C
Image quality	S			
Sky transparency	S			

3.3 New Tracker

The new PFIP is approximately 1000 kg heavier, has a 20% larger diameter, and is 210% taller than the current PFIP. The new PFIP's increased weight and size mandate a larger and stronger tracker. A preliminary design for the new tracker was developed by The University of Texas Center for Electromechanics (CEM) in conjunction with the HETDEX team. CEM is also developing a preliminary design for the fiber management system (FMS) that is used to support the VIRUS IFUs (see Section 4 below).

Figure 3 shows the design that was presented at the PDR. During the design process, a study was conducted to determine the optimal structure for the tracker bridge. The goal was to maximize the natural frequency of the structure, while simultaneously minimizing wind sail area, weight, obscuration of the primary mirror, and critical stresses and deflections. Three different bridge concepts were modeled and analyzed with the PFIP at its worst case location on the tracker. The design based on the Warren truss was selected because it had the best overall performance of the designs studied.

Various hexapod configurations were also studied in an effort to prevent load reversal in the struts as they travel through their full range of motion, and to minimize hexapod positioning errors, stress, deflection and actuator loads. Prior to converging upon a baseline design, approximately 60 iterations were performed to study the parameter space in terms of these performance parameters. The parameter space included: 1) upper and lower hexapod frame cross-sectional characteristics (e.g., I-beam versus open rectangular beams), 2) distance between the upper and lower hexapod frames, 3) location of the upper and lower frame strut attachment points (including varying their angular positioning with respect to the ρ axis), and 4) strut diameter and length.

CEM is using LMS DADS[19] and Simulink® [20] to model the dynamic performance of the tracker and the FMS in the presence of friction and wind-generated forces. The goal is to create an end-to-end dynamic simulator that will be used to:

- Estimate magnitudes of the time-dependent forces generated in the various structures due to tracker motion. This information will be used in conjunction with finite element analysis to ensure that stresses are within safe limits
- Verify that the selected hardware and software will meet performance requirements
- Debug the motor controller motion control system software
- Assign the initial motion control system parameter values that will be refined during integration and testing of the entire tracker at CEM

Initial simulation models have been developed and are being refined as various aspects of the design mature.

3.4 Telescope Structure and Azimuth Bearing Upgrade

The base of the telescope is attached to a pintle bearing (via a flexure) which allows the entire structure to rotate (in azimuth) about a vertical shaft that is anchored in the concrete floor. Additionally, the telescope base has four foot pads that rest on top of a 15 m diameter annular concrete pier. To change azimuth, eight air bearings located adjacent to these pads are used to raise the entire telescope, and then two drive wheels are used to propel the structure to the desired azimuth. The air bearings are currently at capacity and need to be modified to accommodate the additional weight of the

larger corrector, PFIP, tracker and VIRUS spectrographs. An initial design study conducted by General Dynamics SATCOM Technologies (the original supplier of the telescope structure and azimuth drive system), in the first quarter of 2008, suggests that the existing air bearings can be readily replaced with higher capacity bearings, and that the azimuth drive and overall telescope structure will not require any additional modifications to handle the heavier load.

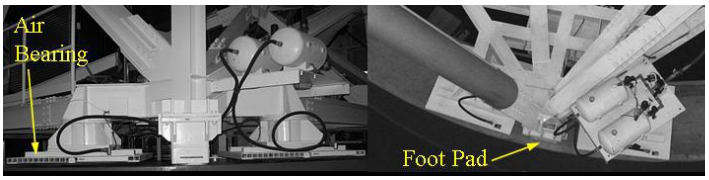

Figure 6. The photograph on the left is a side view of two of the air bearings that are associated with one of the foot pads. The photograph on the right is a top view of this area and shows the annular concrete surface that the air bearings ride on as the telescope is rotated in azimuth.

4. VIRUS

4.1 VIRUS History

The original VIRUS concept was conceived by Gary Hill and Phillip MacQueen and was reported in the literature in 2002.[21] Since its initial inception, VIRUS has evolved from a design utilizing simple refractive optics to one based upon catadioptric optics. This evolution was driven by a need to obtain reasonable throughput at wavelengths down to 350 nm with reasonably-priced optics. Purely refractive designs required a large number of elements and the use of calcium fluoride which is cost prohibitive.

VIRUS consists of multiple simple fiber-fed spectrographs. A prototype spectrograph (referred to as VIRUS-P) was fabricated and has been in use since October 2006, primarily on McDonald Observatory's 2.7 m Harlan J. Smith Telescope (see Figure 7) for a pilot survey to study the properties of Lyman-α emitting (LAE) galaxies which are the focus of the HETDEX survey. Later, in March 2008, it was installed on the HET for the first time to verify predicted sensitivities. Tests conducted with VIRUS-P have yielded excellent data which have been used to confirm the adequacy of the design and to test the data reduction and analysis algorithms. Additional tests are underway with larger fibers and longer fiber bundles to obtain data necessary to finalize the optical design parameters. Additional LAE pilot survey observations are also planned to verify that LAEs are detected at the rate required to complete the HETDEX survey within the anticipated time period.

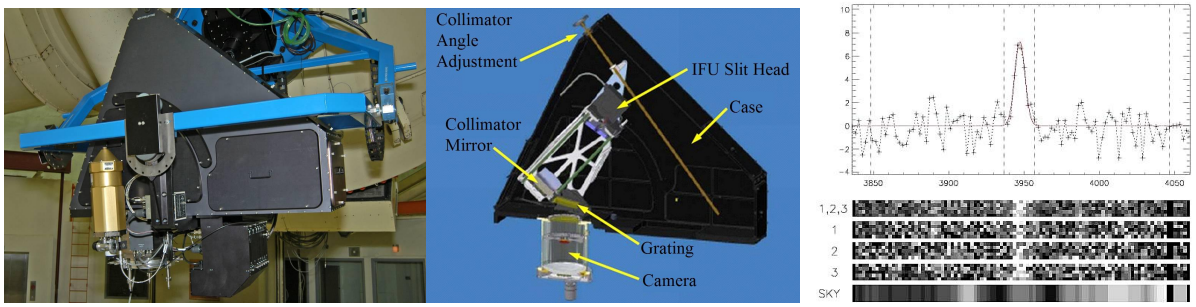

Figure 7. The photograph on the left shows VIRUS-P installed on the Harlan J. Smith telescope. The illustration in the middle shows the interior components which are fed by an IFU that contains 246 fibers with 200 μm diameter cores. A spectrum of a candidate LAE, acquired with VIRUS-P during the pilot survey, is shown on the right.

4.2 VIRUS Design

Evolution of the VIRUS design from the prototype to the production model will be made in two steps. First, a preproduction prototype (VIRUS-PP) will be developed that incorporates the value engineering required to reduce costs. This effort is being performed in collaboration with the Advanced Research Lab at Penn State University. After VIRUS-PP performance is validated on the sky, the design will be modified accordingly, and then production will begin with an initial batch of ten units.

Three significant design changes have already been made to the spectrograph design based upon experience with VIRUS-P and engineering issues discovered while refining the design of the WFU components. The most significant design change is to pair the spectrographs so that they share a single IFU, a common housing, and a common cryostat. The motivation for this has come first from fiber handling: it is more efficient in terms of weight and cross-sectional area

to double the number of fibers in a cable (note that the dominant weight in the bundle is the armored fiber jacket and not the fibers). Additionally the cable handling becomes significantly easier with only 92 cables to accommodate. The other advantage to pairing the spectrographs is that two cameras share a vacuum and have a single connection to the LN cooling system. This reduces system cost because it halves the number of vacuum valves and gauges required.

The second significant change is associated with spectral coverage and fiber diameter. Analysis of the fiber diameter for maximizing the number of LAE galaxies detected by the HETDEX survey indicates that the ideal is 1.5″ for the expected range of image quality to be encountered during the survey (1.3″ to 1.8″ FWHM). Analysis of the expected number of LAEs with redshift also indicates that the majority of the objects are located at $z < 3.5$ due to the change in the distance modulus with redshift coupled with the steepness of the LAE luminosity function. As a result, the decision has been made to reduce the wavelength coverage so as to preserve spectral resolution, while accommodating a reduced number of larger fibers (i.e., 226 fibers with 265 μm diameter cores versus 246 fibers with 200 μm diameter cores).

The third significant change is to modify the optical layout to make the system more linear, thereby allowing the spectrographs to be packed more efficiently in less space.

The baseline VIRUS spectrograph design is shown in Figure 8. The IFU feeds the collimator from the left through a concave cylindrical meniscus lens. Light from the f/3.35 collimator is dispersed by a volume phase holographic (VPH) grating with 930 l/mm. The dispersed light enters the f/1.33 Schmidt camera which contains a cryogenically cooled 2k by 2k back-side illuminated CCD camera with 15 μm by 15 μm pixels. More details can be found in Reference 22.

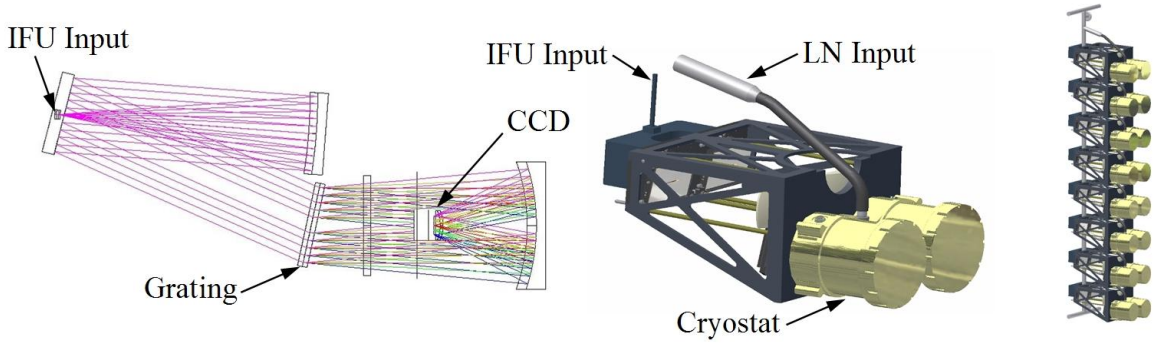

Figure 8. The improved design simplifies IFU cable handling, facilitates tighter packing, and reduces costs associated with vacuum valves and gauges. The illustration on the right depicts the close packing of eight spectrograph pairs.

4.3 VIRUS IFUs

VIRUS is fed by 96 IFUs. Each IFU consists of an input head that is connected to two output heads via an armored fiber optic cable bundle (Figure 9). The input heads are arranged on a rectangular grid oriented so that their optical axes are normal to the WFC's spherical focal surface. Each input head has a rectangular array of 448 fibers which are "split out" of the cable bundle into two linear arrays, each with 224 fibers. This "split out" occurs near the end of the cable bundle that connects to the spectrographs.

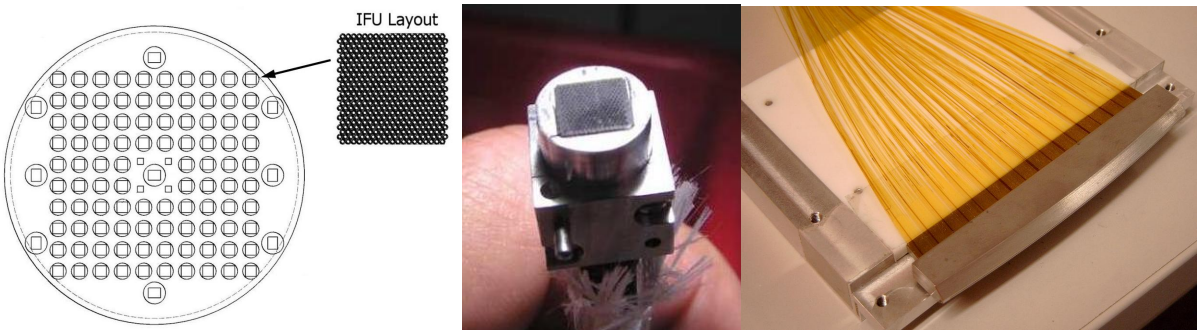

Figure 9. The illustration on the left shows the IFU arrangement at the WFC focal surface. The center photograph is a closeup of a VIRUS-P input head which contains 246 fibers. The photograph on the right illustrates how the fibers are "fanned out" into a linear array at a VIRUS-P output head.

4.4 VIRUS Spectrograph Location

Trade studies aimed at determining the best location for the spectrographs, and how best to manage the fiber optic cable bundles that connect the moving PFIP to the stationary spectrographs, were started early in the project and are progressing. To maximize optical throughput (especially at shorter wavelengths) the IFU cables need to be made as short as possible. The shortest lengths are achieved when the spectrographs are located near the top of the telescope structure. A concept that was presented at the PDR is shown in Figure 10. This design has two strong advantages: it minimizes fiber length, and it prevents wind-induced motion of the spectrograph enclosures (which have an effective wind sail area of 40 m^2) from shaking the PFIP optics and causing image degradation. Unfortunately this concept has several major problems: it is expensive to implement, it increases system complexity, and it limits some man lift access paths to the primary mirror and other parts of the telescope. In addition, since there is limited clearance between the dome interior and top of the telescope, the only safe practical way to provide access to the spectrograph for maintenance is through the addition of an elevating service platform and several auxiliary platforms, which requires substantial modification of the dome ring-wall structure and floor/foundation (that is in the vicinity of the service platform). Other design concepts are currently being explored which offer simpler, more cost-effective solutions to the above-mentioned problems at the expense of increased fiber length. Final trade study results are anticipated by the end of 2008.

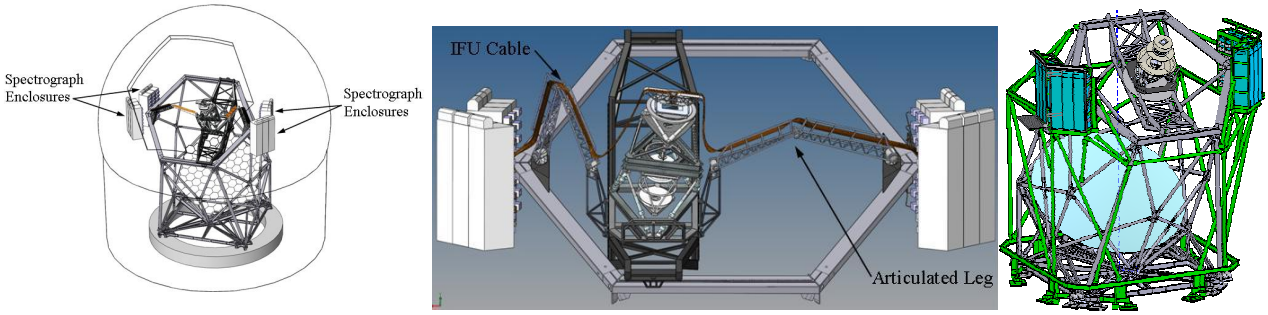

Figure 10. The illustration on the left shows the spectrographs located in 12 environmentally sealed enclosures located near the top of the telescope structure. The center figure illustrates the IFU cable routing between the PFIP and enclosures via the FMS articulated legs, which move with the PFIP as it tracks across the sky. In this figure, the PFIP is shown at one of the extreme ends of its travel limits. The figure on the right shows a spectrograph enclosure support structure that wraps around the existing telescope structure. Since this structure is isolated from the telescope structure, wind-induced motion of the enclosures does not contribute to image quality degradation.

4.5 VIRUS Cryogenic System

Applied Cryogenics Technology was contracted to develop a concept for cooling the VIRUS CCDs. Their study[23,24] was completed in April 2008. A variety of different cryogenic cooling systems and fluids were considered with respect to performance, installation/operational convenience, reliability, capital costs, and operating costs. The study concluded that on-site generation of cryogen cannot compete with liquid nitrogen (LN) delivery (via truck) with regards to cost and reliability. Even the most affordable generation system has a five-year cost (capital and operating) that is approximately 30% higher than liquid delivery at today's diesel fuel prices.

The baseline cryogenic system provides approximately 3600 W of cooling: 2600 W for losses and 960 W to the CCD camera cryostats. The system is reliable and requires minimal maintenance because it has no active moving parts other than servo valves. Additionally, the design allows individual spectrographs to be removed from the system without affecting cooling to the other spectrographs or exposing personnel to LN.

The baseline system (Figure 11) consists of a standard 42000 liter Dewar that supplies LN to the spectrographs via two 160 liter thermal siphons (TSs) and distribution manifolds. The Dewar is located external to the dome and is replenished every two to three weeks from a standard 22700 liter tank truck. The Dewar is connected to the TSs (Figure 11) by approximately 120 m of vacuum-jacketed delivery line. Since the telescope rotates 540° in azimuth, a 20 m portion of the delivery line is flexible to accommodate the cable wrap. As LN boils in the dewar, a pressure of 3 to 4 atmospheres is developed which is sufficient to deliver LN, at the required rate, to the TSs which are located 20 m above the dome floor.

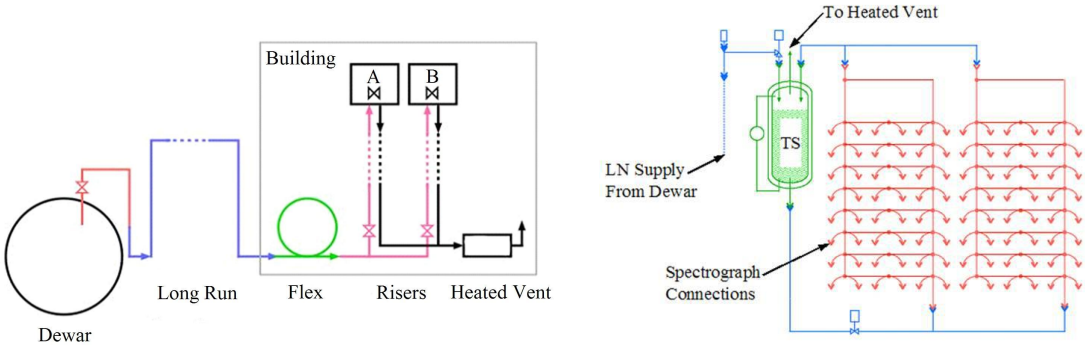

Figure 11. The schematic diagram on the left shows the LN supply system which consists of a large Dewar that is connected to two thermal siphons (shown as items A and B) via a long run of tubing, a shorter run of flexible tubing which traverses the telescope's azimuth cable wrap, and then two 20 m tall risers. The schematic on the right shows how each TS gravity feeds LN to 96 spectrographs via horizontal distribution manifolds fabricated from tube.

Each TS (designated by items A and B in Figure 11) is fed by a separate riser and has a 160 liter capacity. LN contained in the TSs is gravity fed to the spectrographs via 16 horizontal distribution manifolds. The final thermal connection to each spectrograph is via a short length of flexible tube that connects to the camera cryostat via the modified bayonet shown in Figure 12. LN vaporized by the cryostats collects in the top of the TSs and is eventually vented to atmospheric pressure via heated vents connected to the TSs.

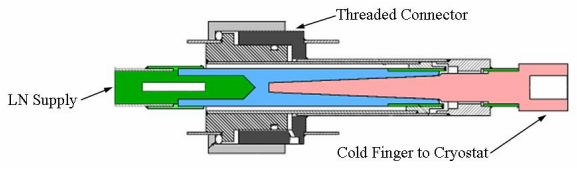

Figure 12. The bayonet design allows the cold finger to be removed from the cryostat receptacle without affecting cooling to the other cryostats or exposing personnel to LN.

The design of the horizontal distribution manifolds and bayonets is unique and will be confirmed before fabrication begins. Experiments with full-scale mockups of the distribution manifolds and prototype bayonets are planned for 2008 to obtain the two-phase flow and critical heat flux data required to complete the design and verify performance.

5. SUMMARY

The HET is undergoing a major upgrade to support the DEX and facilitate large field systematic emission-line surveys of the universe. Table 3 highlights the primary differences between the current and upgraded HET, while Table 1 presents primary advantages of the upgraded system. The project is well under way; a SRR was conducted in June 2007, followed by a PDR in April 2008. Integration and testing is scheduled to begin in November 2009 and will last approximately one year. Installation and commissioning at HET is anticipated to begin in the Fall of 2010 with science observations resuming near the end of 2010.

Table 3. Comparison of the current and upgraded HET.

Item	Current Het	Upgraded HET
Effective focal ratio	4.7	3.65
Field of view	4′	22′
Pupil diameter	9.2 m	10.0 m
WFC protection	None	Air purged
Guide cameras	1 camera	2 cameras
WFS	None	2 sensors
FCU	None	Located below WFC optical entrance window
LRS	Located on PFIP	Relocated to spectrograph room
Rho stage	SAC, DMI, TTCAM and science instruments rotate	Only science instruments rotate
ADC	None	Full and partial field ADCs are being explored
VIRUS	None	Between 150 and 192 spectrographs

REFERENCES

[1] G.J. Hill, K. Gebhardt, E. Komatsu, N. Drory, P.J. MacQueen, J.J. Adams, G.A. Blanc, R. Koehler, M. Rafal, M.M. Roth, A. Kelz, C. Gronwall, R. Ciardullo, D.P. Schneider, "The Hobby-Eberly Telescope Dark Energy Experiment (HETDEX): Description and Early Pilot Survey Results," in "Panoramic Surveys of the Universe," *ASP Conf. Series*, in press

[2] T.A. Sebring, S. Weinberg, J.W. Barna, "West Texas Time Machine – Creating the Hobby-Eberly Telescope," McDonald Observatory

[3] T.G. Barnes, M.T. Adams, J.A. Booth, M.E. Cornell, N.I. Gaffney, J.R. Fowler, G.J. Hill, G.M. Hill, C. Nance, F. Piche, L.W. Ramsey, R.L. Ricklefs, W.J. Spiesman, P.T. Worthington, "Commissioning Experience with the 9.2-m Hobby-Eberly Telescope," Proc. SPIE, **4004**, 14 (2000)

[4] G.J. Hill, P.J. MacQueen, P. Palunas, M.D. Shetrone, J.A. Booth, "Present and Future Instrumentation for the Hobby-Eberly," Proc. SPIE, **6269**, 626907 (2006)

[5] M.J. Wolf, P. Palunas, J.A. Booth, M.H. Ward, A. Wirth, G.L. Wesley, D. O'Donoghue, L.W. Ramsey, "Mirror Alignment Recovery System on the Hobby-Eberly Telescope," Proc. SPIE, **4837**, 714 (2003)

[6] P. Palunas, J.R. Fowler, J.A. Booth, G. Damm, G.H. Ames, "Control of the Hobby-Eberly Telescope Primary Mirror Array with the Segment Alignment Maintenance System", Proc. SPIE, **5496**, 659 (2004)

[7] G. J. Hill, "The Hobby-Eberly Telescope: Instrumentation and Current Performance," in Optical and IR Telescope Instrumentation and Detectors, Proc. SPIE **4008**, 50, 2000

[8] G. J. Hill, P.J. MacQueen, L.W. Ramsey, "Performance of the Facility Instruments on the Hobby-Eberly Telescope," in Optical and IR Telescope Instrumentation and Detectors, Proc. SPIE **4841**, 43, 2003

[9] J.A. Booth, M.J. Wolf, J.R. Fowler, M.T. Adams, J.M. Good, P.W. Kelton, E.S. Barker, P. Palunas, F.N. Bash, L.W. Ramsey, G.J. Hill, P.J. MacQueen, M.E. Cornell, E.L. Robinson, "The Hobby-Eberly Telescope Completion Project," Proc. SPIE **4837**, 919 (2003)

[10] J.A. Booth, P.J. MacQueen, J.M. Good, G.L. Wesley, G.J. Hill, P. Palunas, P.R. Segura, R.E. Calder, "The Wide Field Upgrade for the Hobby-Eberly Telescope," Proc. SPIE **6267**, 62673W (2006)

[11] J.A. Booth, M.T. Adams, E.S. Barker, F.N. Bash, J.R. Fowler, J.M. Good, G.J. Hill, P.W. Kelton, D.L. Lambert, P.J. MacQueen, P. Palunas, L.W. Ramsey, G.L. Wesley, "The Hobby-Eberly Telescope: Performance Upgrades, Status, and Plans," Proc. SPIE **5489**, 288 (2004)

[12] G.J. Hill, P.J. MacQueen, L.W. Ramsey, M.D. Shetrone, "Performance of the Hobby-Eberly Telescope and Facility Instruments," Proc. SPIE **5492**, 94 (2004)

[13] E.S. Barker, M.T. Adams, F. Deglman, V. Riley, T. George, J.A. Booth, A. Rest, E.L. Robinson, "Determination of the Intrinsic Site Seeing for the Hobby-Eberly Telescope," Proc. SPIE **4837**, 225 (2003)

[14] Sagem Défense Sécurité, "Wide Field Corrector Design Study Report," HETDEX HX0020, July 2007

[15] University of Arizona Optical Sciences Center, "Design Study for the Hobby-Eberly Telescope Wide Field Corrector Final Report", HETDEX HX0021, July 2007

[16] J.A. Booth, P.J. MacQueen, J.G. Good, G.L. Wesley, P.R. Segura, P. Palunas, G. J. Hill, R.E. Calder, "Wide Field Upgrade for the Hobby Eberly Telescope," Proc. SPIE, **6267**, 2006

[17] P. Palunas, P.J. MacQueen, J.A. Booth, R. Calder, J.R. Fowler, M.D. Shetrone, S.C. Odewahn, P. Segura, G.L. Wesley, G. Damm, J. Martin, P. Samuel Odoms, "Imaging Performance of the Hobby-Eberly Telescope," Proc. SPIE, **6267**, 2006

[18] M. Lloyd-Hart, "Preliminary Study of Wave-Front Sensing Techniques for Alignment of the Hobby-Eberly Telescope's HETDEX Package," HETDEX HX0024, March 2008

[19] See LMS website at www.lmsintl.com/DADS

[20] See The MathWorks™ website at www.mathworks.com/products/simulink

[21] G.J. Hill, P.J. MacQueen, "VIRUS: An Ultracheap 1000-object IFU Spectrograph," Proc. SPIE, **4836**, 306, 2002

[22] G.J. Hill, "Description of VIRUS," HETDEX HXTR0005, April 2008

[23] Applied Cryogenics Technology, "VIRUS Cryogenic System Study TASK 1B Final Report," HETDEX HX0023, April 2008

[24] M.P. Smith, G.T. Mulholland, J.A. Booth, J.M. Good, G.J. Hill, P.J. MacQueen, M.D. Rafal, R.D. Savage, B.L. Vattiat, "The cryogenic system for the VIRUS array spectrographs on the Hobby-Eberly Telescope", Proc. SPIE, **7018**-117, 2008